

Received March 12, 2020, accepted March 28, 2020, date of publication March 31, 2020, date of current version April 16, 2020.

Digital Object Identifier 10.1109/ACCESS.2020.2984680

A Moving Shadow Elimination Method Based on Fusion of Multi-Feature

HONGRUI ZHANG¹, SHAOCHENG QU¹, (Member, IEEE), HUAN LI², JING LUO¹, AND WENJUN XU¹

¹College of Physical Science and Technology, Central China Normal University, Wuhan 430079, China

²Department of Special Technology, Army Special Operations College, Guilin 541000, China

Corresponding author: Shaocheng Qu (qushaocheng@mail.ccnu.edu.cn)

This work was supported in part by the National Natural Science Foundation of China under Grant 61673190/F030101, and in part by the Self-Determined Research Funds of Central China Normal University (CCNU) from the Colleges' Basic Research and Operation of the Ministry of Education (MOE) under Grant CCNU18TS042.

ABSTRACT Moving shadow elimination plays an important role in the field of moving object detection. However, the accuracy of shadow elimination is an open question, due to illumination and complex texture. Furthermore, the problem of misclassification of moving object caused by shadow has also become increasingly serious. To address this problem, this paper presents a moving shadow elimination algorithm based on the fusion of multi-feature pattern, which can enhance the accuracy of moving object detection system. In this approach, a dual-channel HSV color space feature and a uniform extended scale invariant local ternary pattern (UESILTP) texture feature are synthesized to elimination shadow. It greatly overcomes the misjudgment of dark object by color feature and the false detection caused by inconspicuous texture characteristics of moving object. Meantime, a method of region growth is adopted to fill the existing cavities in the color space. Finally, qualitative and quantitative comparisons with state-of-the-art methods show that the algorithm is effective.

INDEX TERMS Shadow elimination, HSV, region growth, UESILTP.


I. INTRODUCTION

The purpose of moving object detection is to extract the foreground area in the video sequence, which is widely used in video surveillance, traffic detection, navigation, and other fields.

At present, the methods for moving object detection mainly contain background subtraction method [1], [28], optical flow method [2], [27], frame difference method [3]. The background subtraction method has been intensively investigated. It uses a parameter model of the background to approximate pixel values of the background image, differentiates the current frame from background image, and then selects an appropriate threshold to compare the obtained pixels with the threshold to obtain moving objects. The optical flow method describes each pixel in the image as a velocity vector to approximate the motion field. The frame difference method determines moving objects by judging gradation difference of the pixel points corresponding to the two frames before and after. However, the above three moving object detection

methods are subject to the shadow problem caused by illumination, which will affect the accuracy of subsequent video processing, such as target tracking and recognition. Therefore, an effective method of shadow elimination is crucial for moving object detection.

During the past decade, a variety of moving shadow elimination algorithms continually spring up. Usually, these methods are mainly divided into four categories: geometry-based methods [4], [22], texture-based methods [5], [29], [30], chromaticity-based methods [6], [31], and physical model-based methods [7]. Geometry-based methods assume that light source, object shape, and the ground plane are known, using the information of direction, size, and shape of shadows to detect shadows [8]. Texture-based methods use the characteristic that texture features of the background region remain unchanged after being covered by shadows. Chromaticity-based methods utilize the feature that when shadows cover the background area, the brightness value and saturation of the area change greatly, but the hue changes little to detect shadows. Physical model-based methods model the shadows with various light sources in mind. Currently, with the continuous development of deep learning, a convolutional

The associate editor coordinating the review of this manuscript and approving it for publication was Xian Sun .

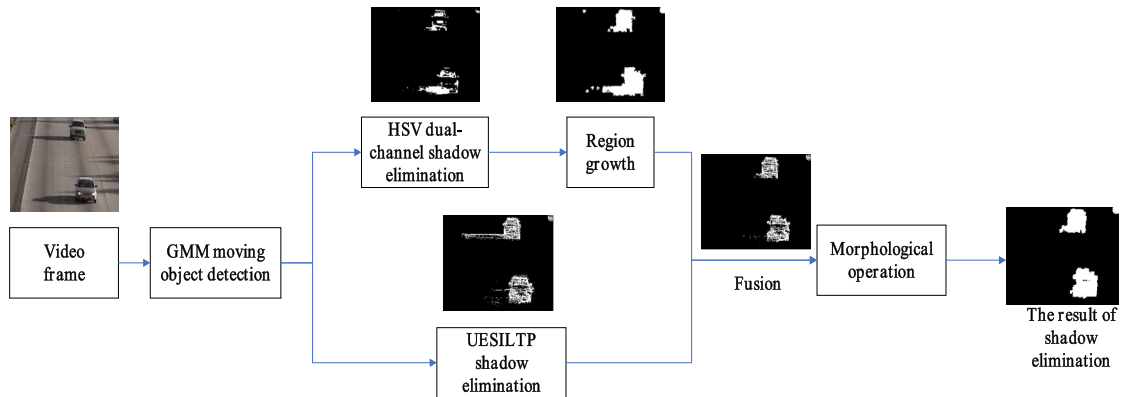


FIGURE 1. The framework of the moving shadow elimination.

neural network has attracted much attention in the field of moving shadow detection and elimination. This method can extract features through automatic learning.

Among the methods mentioned above, single-feature based methods, for example, chromaticity-based methods have a faster processing speed, but this method is sensitive to changes in illumination. Texture-based methods are robust to illumination changes, but the calculation speed is slow. The method based on multi-feature is better than single-feature in detection accuracy. However, the calculation speed is slower than single-feature. The model obtained by the deep learning method can be better applied to another scene, but a large amount of labeled data needs training, which is pretty time-consuming. Moreover, shadow elimination based on deep learning is mainly concentrated on a single image, and there is less research on the elimination of moving shadows. The main reason is the time variability of moving shadows. Hence, after comprehensive consideration, this paper uses a new method based on multi-feature fusion to eliminate shadows. The main contributions of this paper are as follows:

- (1) The dual-channel HSV color feature method is proposed for shadow elimination, which reduces the amount of calculation and obtains shadow elimination effect.
- (2) UESILTP texture feature is proposed to eliminate shadows, and experiment shows that the accuracy of shadow descriptions is improved by acquiring more image local feature information.

The framework of the proposed method is shown in Figure 1. In the first place, the moving object is obtained by applying GMM. Then, shadow elimination using dual-channel HSV color space feature and UESILTP texture feature, respectively. Finally, the aforementioned shadow elimination experimental results are fused, and a complete moving object is obtained by morphological processing.

The structure of the article is as follows. Section II introduces the methods associated with shadow elimination. Section III describes the detailed elaboration about moving object detection based on GMM. Section IV explains the integrated shadow elimination of the dual-channel HSV color

space feature and UESILTP texture feature. The comparative experimental results of the public video set with the proposed algorithm and the existing algorithm are given in section V, and the conclusions are given in Section VI.

II. RELATED WORK

In this section, we will detail the work on moving shadow elimination.

Chromaticity-based methods: Cucchiara *et al.* [6] employed the chromaticity and luminosity information separated by HSV color space to establish a mathematical formula for shadow detection. Chen *et al.* [9] presented an enhanced segmentation method in YUV color space, which can reduce the interference of shadows for moving object detection. Sun and Li [10] performed shadow detection in the HSI and c1c2c3 combined color model. This model used the ratio of hue over intensity and the theory of photometric color invariants to achieve the purpose of eliminating shadows. Khare *et al.* [11] adopted the Daubechies complex wavelet transform to eliminate shadows in HSV color space.

Texture-based methods: Zhang *et al.* [12] used local binary pattern (LBP) to obtain texture features of shadow regions. Leone and Distanto [13] proposed a texture compression representation method based on Gabor function decomposition coefficients, and conducted shadow detection by evaluating the similarity between texture patches. Wang and Chen [14] introduced an approach for distinguishing shadows based on homomorphic filtering and scale-invariant local ternary pattern.

Geometry-based methods: Hsieh *et al.* [15] employed the Gaussian shadow modelling to make use of multiple features of the shadow region, such as orientation, mean intensity, center position, to perform shadow reduction from coarse to fine. The innovation of Chen and Aggarwal [8] shadow elimination method was the presentation of multicue shadow descriptors.

Physics-based methods: Nadimi and Bhanu [16] designed a new physical model based on blue ratio test and albedo ratio segmentation. Joshi and Papanikolopoulos [17]

proposed a moving shadow detection method based on support vector machine and cooperative training algorithm. Huang and Chen [7] showed an online statistical learning method to simulate changes in the background under the shadow without prior consideration of illumination.

Deep learning-based methods: Lee *et al.* [23] used superpixels extracted via energy-driven sampling and convolutional neural networks to perform moving shadow detection. Khan *et al.* [24] designed a framework that used convolutional neural networks to learn features of superpixels and object boundaries. Hu *et al.* [25] constructed a direction aware attention mechanism in spatial recurrent neural networks to detect shadows. The last two pieces of literature are related to shadow elimination for a single image.

Among the above-mentioned methods, multi-feature shadow detection and elimination method based on combination of color feature and texture feature is widely used. Xie *et al.* [18] described a histogram of regional gradient direction to describe texture feature and then combined the color feature to detect shadows. Dai *et al.* [19] combined HSV color feature and LBP feature to eliminate shadows. Qin *et al.* [20] adopted SILTP feature and RGB feature, and introduced an online learning scheme that can cope with environmental changes.

III. GMM MOVING OBJECT DETECTION

Background subtraction based on GMM (Gaussian mixture model) is the most representative model. It is particularly attractive as an approach for moving object detection, due to it can deal with gradual changes in illumination and a small amount of repetitive motion of the background.

The GMM gave the characteristics of each pixel in the image by K (usually 3 to 5) Gaussian models [26]. For the pixel $I(x, y)$, assuming the sequence of values at time t is $\{X_1, X_2, \dots, X_t\} = \{I(x, y, i) | 1 \leq i \leq t\}$, the probability that a pixel belongs to X_t is assumed to be:

$$P(X_t) = \sum_{k=1}^K \omega_{k,t} * \eta(X_t, \mu_{k,t}, \sum_{k,t}) \quad (1)$$

where $\omega_{k,t}$ is the weight of the k th Gaussian model, $\mu_{k,t}$ is the mathematical expectation of the k th Gaussian model, $\sum_{k,t}$ is the covariance matrix of the k th Gaussian model, η is Gaussian probability density function, and

$$\eta(X_t, \mu_{k,t}, \sum_{k,t}) = \frac{1}{(2\pi)^{\frac{n}{2}}} e^{-\frac{1}{2}(X_t - \mu_t)^T \sum^{-1}(X_t - \mu_t)} \quad (2)$$

To simplify the calculation, take K as three and assume that the RGB color channels are independent of each other, then the covariance matrix is given as

$$\sum_{k,t} = \delta_{k,t}^2 I \quad (3)$$

Then, compare the current pixel with K Gaussian models to determine whether they are matching or not. If they are a match, the pixel belongs to background. Otherwise, it is

foreground. After matching, the model weights need to be updated, which are expressed as

$$\begin{aligned} \mu_t &= (1 - \rho)\mu_{t-1} + \rho X_t \\ \delta_t^2 &= (1 - \rho)\delta_{t-1}^2 + \rho(X_t - \mu_t)^T (X_t - \mu_t) \\ \rho &= \alpha \cdot \eta(X_t, \mu_t, \delta_t) \end{aligned} \quad (4)$$

where α is the learning rate of the model.

If there is no matching Gaussian component between the current pixel and the K known Gaussian distributions, a Gaussian distribution should be reconstructed. Then, the K Gaussian distributions are downgraded sort according to ω_k/δ_k , finally, the background pixel model is determined by the first L gaussian distributions.

$$L = \arg \min_b \left(\sum_{j=1}^b \omega_j > T \right) \quad (5)$$

where T is the background model threshold. More details about GMM can be obtained from literature [32].

IV. SHADOW ELIMINATION

With the development of video surveillance technology, the requirements for moving object detection has become increasingly higher. Furthermore, if the object is accompanied by casting shadows and noise, which makes the object detection extremely difficult. In order to get the correct object, this paper considers two features of color and texture.

A. SHADOW ELIMINATION IN COLOR SPACE

When shadows cover the background area, the brightness value and saturation of the area are significantly changed. However, the hue changes little. As the above description, we can make use of the above two properties to select appropriate color space for shadow elimination. Compared with the RGB model [6], the HSV model is more closely matched to the human visual system and can directly reflect brightness information of color. Consequently, the color space of HSV is introduced in this paper. Color parameters in the HSV model include hue, saturation, and brightness. Setting these three parameters can achieve the purpose of eliminating shadows, the expression is as follows

$$sp(x, y) = \left\{ \begin{array}{l} 1, \beta \leq \frac{V_C(x, y)}{V_B(x, y)} \leq \gamma \\ \cup |H_C(x, y) - H_B(x, y)| \leq T_H \\ \cup (S_C(x, y) - S_B(x, y)) \leq T_S \\ 0, \text{ otherwise} \end{array} \right\} \quad (6)$$

where $H_C(x, y)$, $S_C(x, y)$, $V_C(x, y)$ are the H , S , and V components of the current frame pixel, respectively. $H_B(x, y)$, $S_B(x, y)$, $V_B(x, y)$ are the H , S , and V components of the background pixel, respectively. When $sp(x, y)$ is 1, it indicates that the pixel is a shadow. In contrast, it belongs to object. T_H and T_S represent the threshold of difference between hue and saturation, respectively. β is associated with the intensity of shadows, and γ is connected with the intensity of light.



(a)input frame (b) H, S, V three-channel experimental result (c)S, V dual-channel experimental result

FIGURE 2. Detection results in HSV color space.

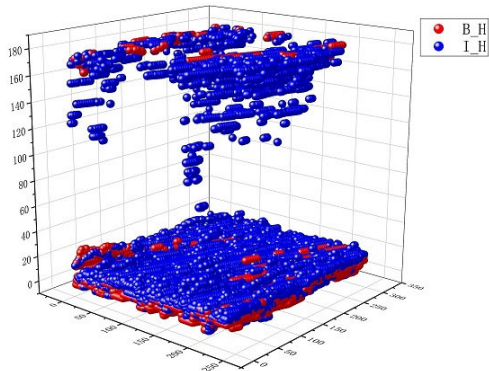


FIGURE 3. H channel pixel hue values in the current frame and background.

According to the characteristic that the hue changes little after objects are covered by shadows. This paper proposes to simplify the three-channel to dual-channel. The shadow elimination results of three-channel of H , S , V , and dual-channel of S and V are given in Figure 2. Figure 3 is the statistics of the current frame (Figure 2(a)) H channel pixel hue value I_H and background H channel pixel hue value B_H , a total of 76,800 pairs of pixels. As can be seen from Figure 2 and Figure 3, there is a little difference between the detection effects of the two. Moreover, the number of changes in the hue value is tiny. Thus, the proposed method is feasible, not only obtains reliable objects, but also reduces the amount of calculation. The shadow discrimination of dual-channel is defined as

$$sp(x, y) = \left\{ \begin{array}{l} 1, \beta \leq \frac{V_C(x, y)}{V_B(x, y)} \leq \gamma \\ \cup (S_C(x, y) - S_B(x, y)) \leq T_S \\ 0, otherwise \end{array} \right\} \quad (7)$$

where $S_C(x, y)$, $V_C(x, y)$ are the S , and V components of the current frame pixel, respectively. $S_B(x, y)$, $V_B(x, y)$ are the S , and V components of the background pixel, respectively. If the saturation and brightness conditions in formula (7) are both satisfied, $sp(x, y)$ is equal to 1. In other words, this pixel is a shadow. In contrast, it is an object.

It can be seen from Figure 2 that after eliminating shadow, the obtained moving objects have large-area cavities. To fill

the cavities, region growth is introduced. The core idea of region growth is to merge the pixels with similar properties.

For each region, a seed point is designated as the starting point for growth. Then, pixels in the neighborhood of the seed point are compared with seed point. Finally, combine points with similar properties. For the sake of visually describe the region growth process, an example of region growth is given in Figure 4. It is illustrated by the example of four-neighborhood, if 45 is selected as the seed point, first of all, the absolute value of the difference between seed point and four neighborhood pixel values is compared with the threshold (assuming the threshold th is 1). Afterwards, if it is less than the threshold, grow in the direction of the pixel. The final result is shown in the right panel of Figure 4. Moreover, the result of region growth obtained from Figure 2(c) is indicated in Figure 5.



FIGURE 4. An example of region growth.



FIGURE 5. Result with region growth.

B. SHADOW ELIMINATION IN TEXTURE SPACE

According to shadow area and background area have similar texture information, this paper chooses to use the texture feature to eliminate moving shadows. In the early stages of research, the LBP texture feature was used for shadow elimination. But, for the sake of making image local texture

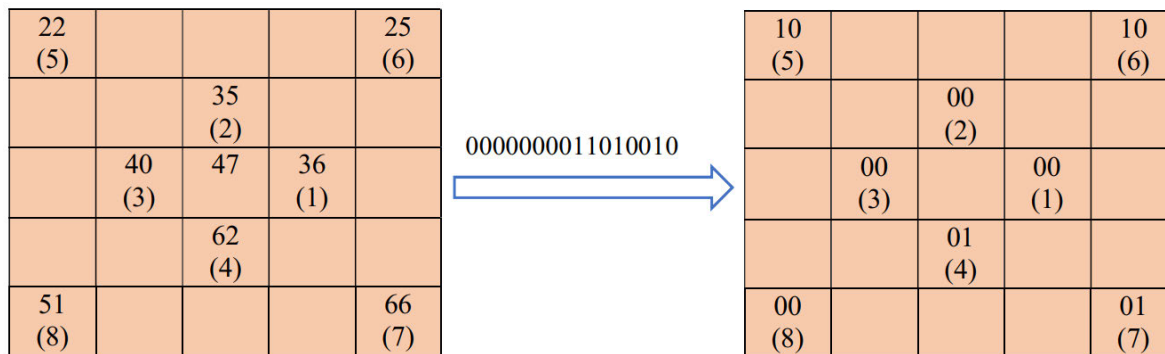


FIGURE 6. An example of ESILTP encoding ((1)~(8) is the connection order).

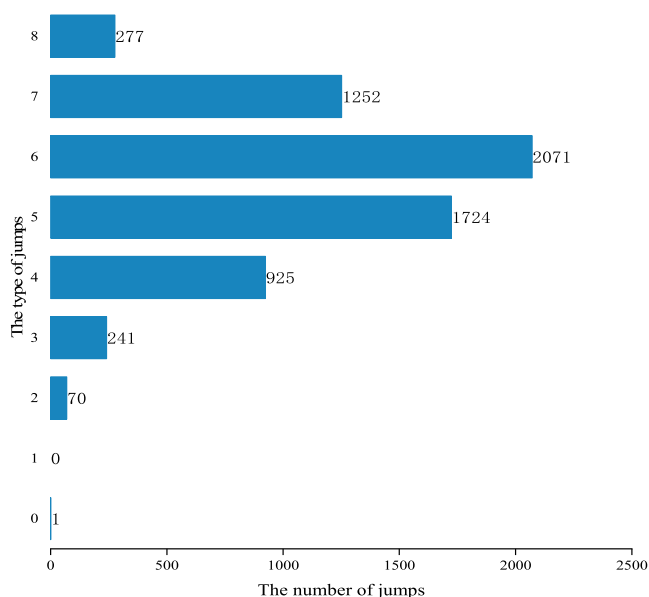


FIGURE 7. ESILTP eigenvalues jump distribution.

features more robust to illumination changes and noise, scholars have continuously improved on LBP. The Ref. [20] introduced SILTP texture feature to address the sudden changes of grayscale intensities. The SILTP feature compares grayscale changes of the central pixel and neighboring pixels in a 3×3 size window. It contains only a small amount of local structural information for the entire image and does not express the local overall feature of the image well. Hence, we extend the window area to a neighborhood size of 5×5 , and the neighboring pixels of eight positions are uniformly and symmetrically selected around the central pixel for threshold comparison, as shown in Figure 6. In addition, the connection sequence as shown in (1) to (8) in Figure 6. According to the above rules, the final value is 0000000011010010. There are 3^8 corresponding eigenvalues. When more local structure information is obtained, the computational complexity of the histogram is increased. In consequence, this paper put forward to use the uniform

TABLE 1. The eigenvalues corresponding to the partial jump types.

Type of jump	ESILTP eigenvalues
0	0000000000000000
1	nothing
2	$\begin{array}{cccccccc} & \rightarrow & \rightarrow & & & \rightarrow & \rightarrow & \\ 00000000 & 0010 & 000 & & 000000 & 0100 & 00000000 & \\ & & & & & \rightarrow & & \\ & & & & & 00000000 & 000000 & 001 \end{array}$
3	$\begin{array}{cccccccc} & \rightarrow & \rightarrow & & & \rightarrow & \rightarrow & \\ 0001100 & 000000000 & & & 000000000000 & 01001 & & \\ & & & & & \rightarrow & \rightarrow & \rightarrow \\ & & & & & 00000000 & 0100 & 100 \end{array}$
4	$\begin{array}{cccccccc} & \rightarrow & \rightarrow & & \rightarrow & & \rightarrow & \rightarrow \\ 0000010 & 000000 & 010 & & 000000 & 0101 & 0000 & 100 \\ & & & & & \rightarrow & \rightarrow & \rightarrow \\ & & & & & 000010 & 00 & 0100 & 000 \end{array}$

pattern for dimensionality reduction. The encoding function of ESILTP is given in the formula (8), and the eigenvalues $ESILTP^\tau(x_c, y_c)$ is defined as the formula (9)







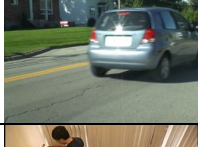

$$S_\tau(I_c, I_n) = \begin{cases} 01, I_n > (1 + \tau)I_c \\ 10, I_n < (1 - \tau)I_c \\ 00, \text{otherwise} \end{cases} \quad (8)$$

$$ESILTP^\tau(x_c, y_c) = \bigoplus_{n=0}^7 S_\tau(I_c, I_n) \quad (9)$$

where τ denotes the scale factor, I_c is the central pixel value, I_n is the neighborhood pixel value. According to formula (8), compare current pixel value with neighborhood pixel value to obtain the corresponding $S_\tau(I_c, I_n)$, then, the eigenvalues are calculated by the formula (9).

The UESILTP uniform pattern classifies ESILTP eigenvalues according to the number of jumps, and the type of binary pattern is greatly reduced without losing any information. The patterns of the ESILTP feature are 6561. For a binary encoding of ESILTP ternary eigenvalue, every two bits are treated as a group. If the encoding between two consecutive

TABLE 2. The details of video sequences.

Video	Scenes	Scene type	Size	Number of frames	Shadow strength	Object type	Object size
	HighwayI	Outdoor	320×240	400	Strong	Vehicle	Large
	HighwayII	Outdoor	320×240	500	Medium	Vehicle	Small
	Campus	Outdoor	352×288	1180	Weak	Vehicle/People	Large
	Laboratory	Indoor	320×240	887	Weak	People/Other	Medium
	Intelligent-room	Indoor	320×240	300	Weak	People	Medium
	backdoor	Outdoor	320×240	2000	Medium	People	Medium
	bungalows	Outdoor	360×240	1700	Strong	Vehicle	Large
	copy-Machine	Indoor	720×480	3400	Weak	People	Medium

(or the head and the tail) groups are different, it is recorded as a jump, such as 00 and 01, 00 and 10, 10 and 01. In accordance with the uniform pattern, there are nine types of jumps: jumping 0 times to jumping 8 times. The eigenvalues corresponding to the partial jump types are given in Table 1, the rest can be done in the same manner. The ESILTP eigenvalues jump types and the number of jumps is indicated in Figure 7. It is obtained through the 6561 patterns of ESILTP. In the bar chart of Figure 7, the number of jumping 0 times to eight times is 1, 0, 70, 241, 925, 1724, 2071, 1252, 277, respectively. However, the UESILTP feature proposed in this paper retains only some eigenvalues. The rules are as follows: First, 1237 eigenvalues of 0 jumps, 2 jumps, 3 jumps, and 4 jumps are reserved, and then the rest of the jumps are classified into

one, thus making the original ESILTP dimension is reduced from 6561 to 1238. Figure 8 is a UESILTP texture feature of Figure 2(a).

V. EXPERIMENTS & ANALYSIS

A. DATA SET AND EVALUATION METRICS

Eight public video sequences are used to test the effectiveness of the proposed algorithm. The detailed information of the video sequences used is shown in Table 2 include indoor and outdoor, strong shadow and weak shadow, different types of test objects. In addition, the commonly used quantitative evaluation metrics include shadow detection rate η [21], shadow discrimination rate ξ [21], comprehensive evaluation

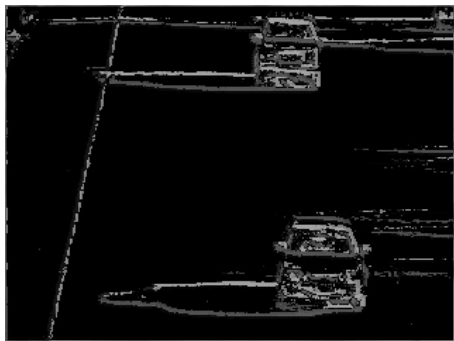


FIGURE 8. UESILTP texture feature of the image.

index Avg [19], and running time. The formulas are given by (10), (11), (12).

$$\eta = \frac{TP_S}{TP_S + FN_S} \tag{10}$$

$$\xi = \frac{TP_F}{TP_F + FN_F} \tag{11}$$

$$Avg = \frac{\eta + \xi}{2} \tag{12}$$

where, TP_S indicates the number of shadow pixels detected correctly, the FN_S denotes the number of shadow pixels that are misclassified, the TP_F indicates the number of foreground pixels detected correctly, and FN_F represents the number of foreground pixels that are misclassified.

B. EXPERIMENTAL RESULTS

In this section, the algorithm of this paper is compared with references 6, 7, 14, 15, 20 and 23. Experiments are implemented by Python 3.7 on a PC with 8 GB RAM, and

Intel i5 processor. The experimental parameters are set to: $K = 3, T = 25, \beta = 0.65, \gamma = 1, T_S = 46, \tau = 0.3, th = 1$.

For the selection of parameters, this section uses the comprehensive evaluation index Avg for analysis. The results are shown in Figure 9. It can be seen from the figure that the effect is better when $\beta = 0.65, \gamma = 1, T_S = 46, \tau = 0.3$, and $th = 1$. The other two parameters K and T use typical values in GMM.

The moving shadow elimination experimental results on different algorithms are given in Figure 10. The videos used in sequence from (a) to (j) are (a)-HighwayI, (b)-HighwayII, (c)(d)-Campus, (e)-Laboratory, (f)-Intelligentroom, (g)-backdoor, (h)-bungalows, (j)-copyMachine. The ground truth given in the figure is obtained by manual segmentation, in which the white part is a moving object and the dark gray part is a shadow. For video backdoor, bungalows, copyMachine, we select the first 1500 frames, 300 frames, and 700 frames for experimental analysis, respectively. In addition, the campus video extracts two types of objects for experimentation, such as people and vehicles. Specifically, (i)-input frame of eight different sequences, (ii)-ground truth, and (iii)~(ix) are the experimental results obtained by the algorithms proposed in literature [6], [7], [15], [20], [14], [23] and the proposed algorithm in this paper, respectively.

We observe the experimental results (iii), (iv), (v). The results obtained from [6], [7], [15] have problems of large cavities and incomplete shadow elimination. For the literature [20], [14], [23] and the method in this paper, it can be seen from the experimental results (vi), (vii), (viii), (ix) that the obtained moving objects are more complete and the shadow elimination effect is good. In addition, the proposed method is superior to the methods used in [20], [14], [23] in terms

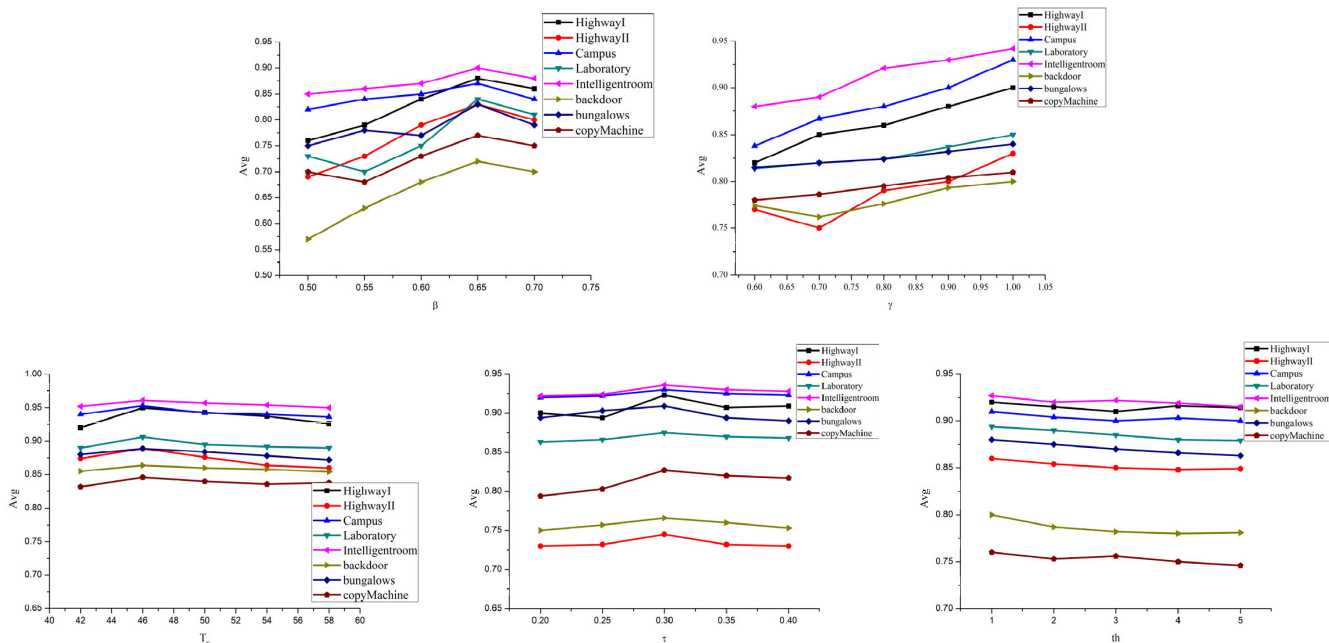


FIGURE 9. The results of parameter selection.

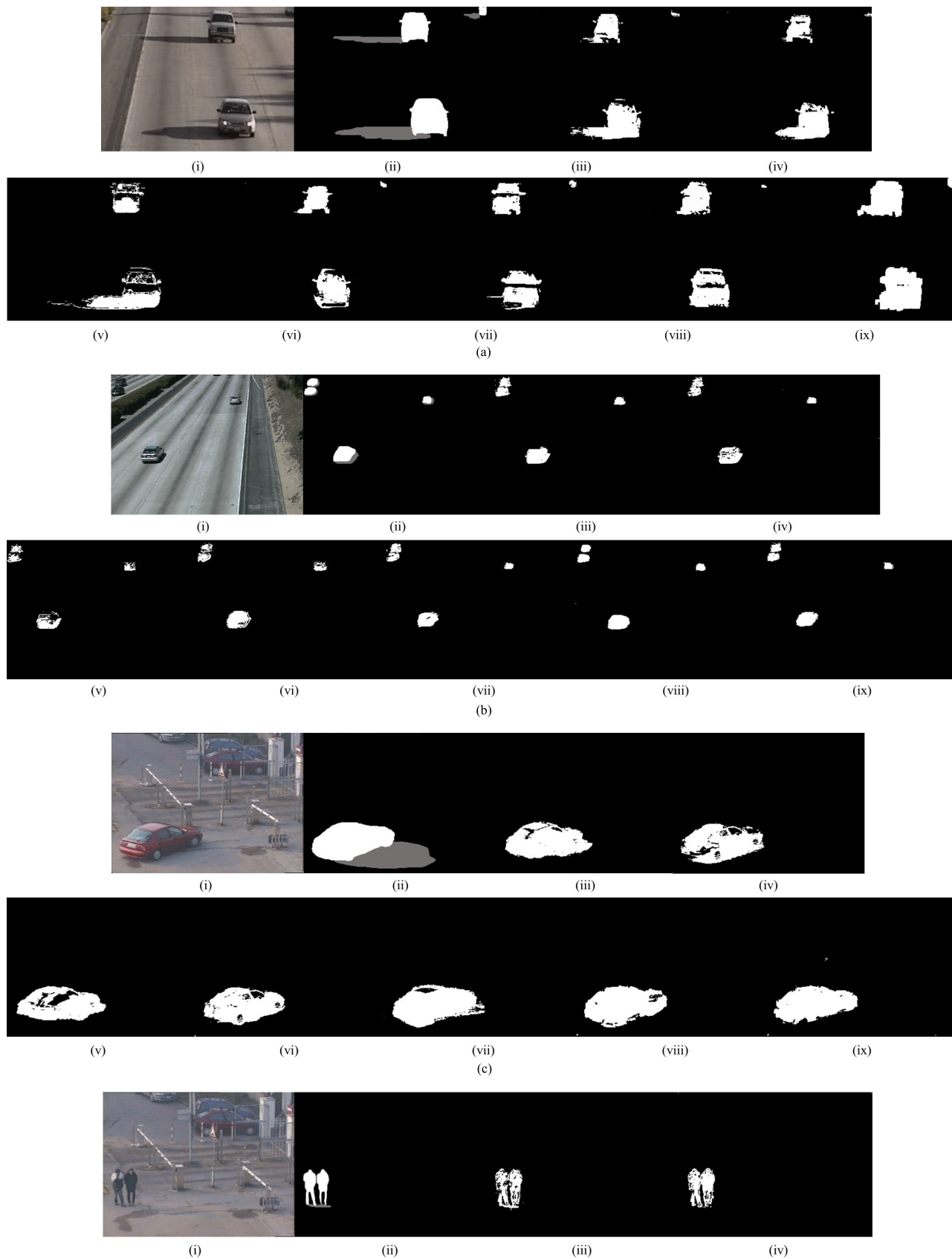


FIGURE 10. Shadow elimination results of different algorithms. [(iii) Cucchiara [6], (iv) Huang [7], (v) Hsieh [15], (vi) Qin [20], (vii) Wang [14], (viii) Lee [23], (ix) our method].

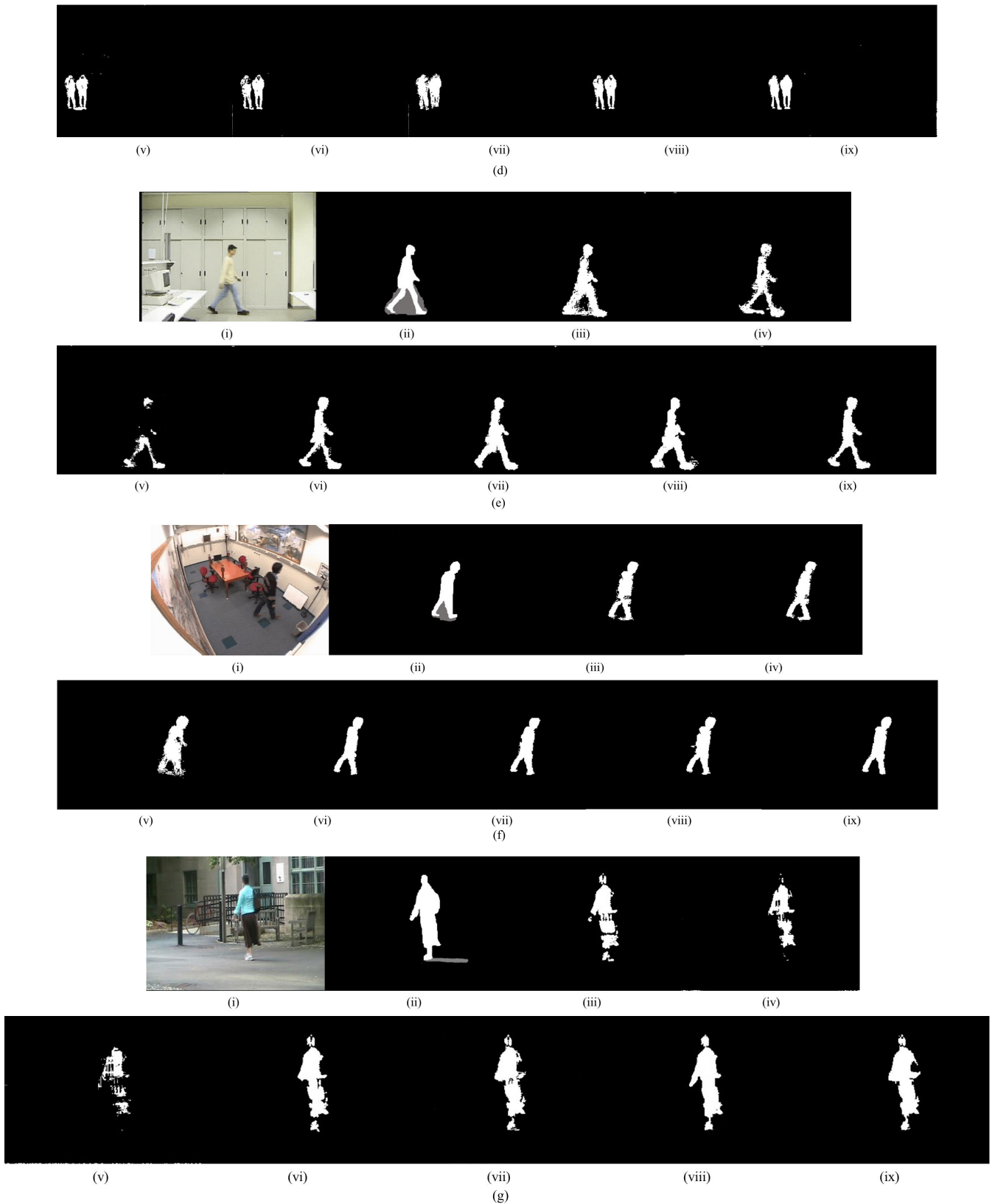


FIGURE 10. (Continued.) Shadow elimination results of different algorithms. [(iii) Cucchiara [6], (iv) Huang [7], (v) Hsieh [15], (vi) Qin [20], (vii) Wang [14], (viii) Lee [23], (ix) our method].

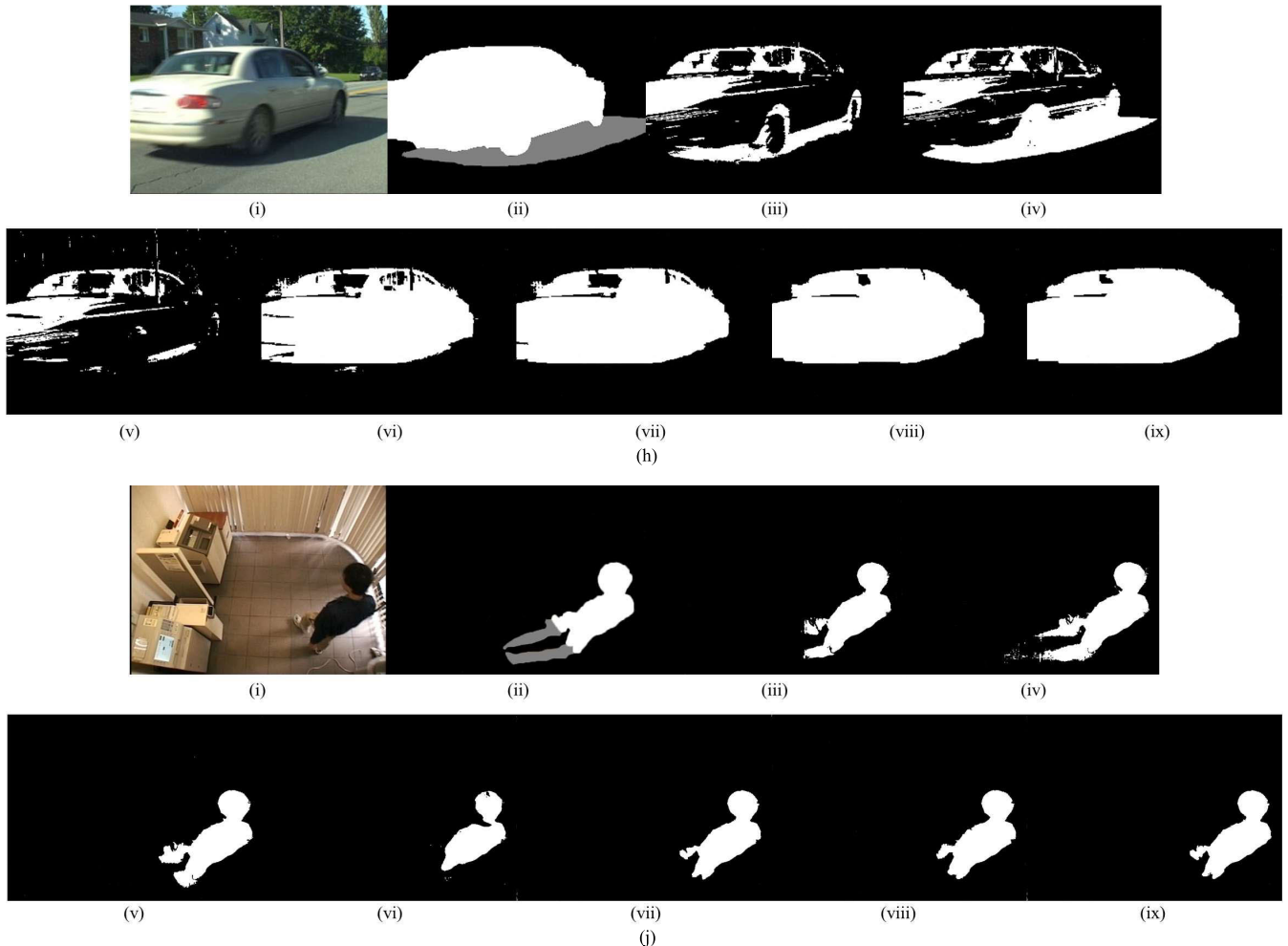


FIGURE 10. (Continued.) Shadow elimination results of different algorithms. [(iii) Cucchiara [6], (iv) Huang [7], (v) Hsieh [15], (vi) Qin [20], (vii) Wang [14], (viii) Lee [23], (ix) our method].

of object integrity and shadow elimination effect. Besides, the method used in [23] requires sufficient labeled training data to guarantee the accuracy of the results.

By observing the experimental results, it can be assumed that the proposed algorithm reveals the ability of shadow elimination, which can acquire more complete moving objects, especially in the face of weaker shadows. Hence, moving objects can be easily separated from the background. It is worth noting that Figure 10[(vi), (vii), (ix)] are the experimental results obtained by combining color feature and texture feature. These results imply that a comprehensive strategy using color feature and texture feature can achieve better results in respect of moving shadow elimination.

At the same time, we use quantitative analysis to comprehensively evaluate the proposed algorithm in this paper. Values of shadow detection rate η , shadow discrimination rate ξ , and comprehensive evaluation index Avg for different methods are shown in Table 3. As a rule, the higher value of η , ξ , and Avg are, the better performance of the method will be. Figure 11 shows the bar chart distribution of the comprehensive evaluation index Avg . The abbreviations of video names

are used in Figure 11, which are HighI-HighwayI, Campus-Campus, HighII-HighwayII, Lab-Laboratory, Introom-Intelligentroom, b-door-backdoor, copmac-copyMachine. It can be seen from Table 3 and Figure 11 that the proposed method shows better performance than other methods. For the literature [14], [20] using the same strategy (color feature and texture feature), the average detection rate of the proposed algorithm in this paper is increased by 0.46%~9.69%.

Besides, as for the computational complexity of the different methods, we use running time as a measure. Table 4 shows the running time of eight video sequences using different approaches. As we can see that the calculation time of the proposed algorithm is a little long. However, compared with the SILTP algorithm used in Ref. [20], the calculation time is greatly improved. Since the SILTP feature selection is in a 3×3 window, the central pixel is compared to its eight neighborhoods, for a total of 3^8 patterns. In this paper, the 5×5 size window is used, and eight local neighbor pixels are uniformly and symmetrically selected around the central pixel, which can obtain more local information. After the dimension reduction processing, the patterns are reduced to 1238, which speeds up the calculation. Although the

TABLE 3. Quantitative comparison results.

Video		HighwayI	HighwayII	Campus	Laboratory	Intelligentroom	backdoor	bungalows	copymachine
Cucchiara et al. [6]	η	73.65	68.24	58.64	69.53	85.67	64.12	63.17	59.64
	ξ	75.41	62.06	66.68	82.46	82.77	62.05	70.54	63.78
	Avg	74.53	65.15	62.66	76.00	84.22	63.09	66.86	61.71
Huang et al. [7]	η	72.84	73.46	80.63	79.75	82.38	68.43	69.44	73.44
	ξ	82.36	71.19	76.49	83.68	85.62	71.95	76.85	64.32
	Avg	77.60	72.33	78.56	81.72	84.00	70.19	73.15	68.88
Hsieh et al. [15]	η	70.21	60.47	67.59	56.43	74.82	69.87	68.96	70.54
	ξ	72.37	70.46	54.74	70.28	86.04	68.86	72.87	75.38
	Avg	71.29	65.47	61.17	63.36	80.43	69.37	70.92	72.96
Qin et al. [20]	η	80.62	75.77	83.68	86.32	89.26	78.45	72.36	74.62
	ξ	90.60	83.25	92.87	89.72	95.43	82.31	83.77	80.41
	Avg	85.61	79.51	88.28	88.02	92.35	80.38	78.07	77.52
Wang et al. [14]	η	83.94	79.34	82.65	87.74	88.91	79.43	78.95	77.89
	ξ	92.47	89.96	94.25	90.78	95.11	83.62	86.43	80.63
	Avg	88.21	84.65	88.45	89.26	92.01	81.53	82.69	79.26
Lee et al. [23]	η	82.47	84.65	84.93	86.47	85.43	85.37	80.91	73.84
	ξ	90.68	94.23	93.62	85.33	90.26	89.24	84.75	80.96
	Avg	86.58	89.44	89.28	85.90	87.85	87.31	82.83	77.40
Proposed method	η	86.06	82.47	85.41	88.27	89.86	79.43	87.05	80.36
	ξ	93.52	91.34	96.60	91.17	96.74	84.65	88.47	82.86
	Avg	89.79	86.91	91.01	89.72	93.30	82.04	87.76	81.61

TABLE 4. The running time of different methods (second).

Video	HighwayI	HighwayII	Campus	Laboratory	Intelligentroom	backdoor	bungalows	copymachine
Cucchiara et al. [6]	0.83	0.91	1.02	0.97	0.50	0.72	0.68	0.95
Huang et al. [7]	0.66	0.69	0.77	0.63	0.53	0.81	0.56	0.74
Hsieh et al. [15]	0.78	0.82	1.06	0.94	0.45	0.85	0.52	0.82
Qin et al. [20]	1.42	1.48	2.15	1.85	1.14	1.96	1.04	1.57
Wang et al. [14]	1.02	1.08	1.69	1.37	0.74	0.94	0.71	1.13
Lee et al. [23]	0.41	0.38	0.72	0.57	0.31	0.49	0.43	0.62
Proposed method	0.83	0.74	1.13	0.98	0.62	0.80	0.65	0.84

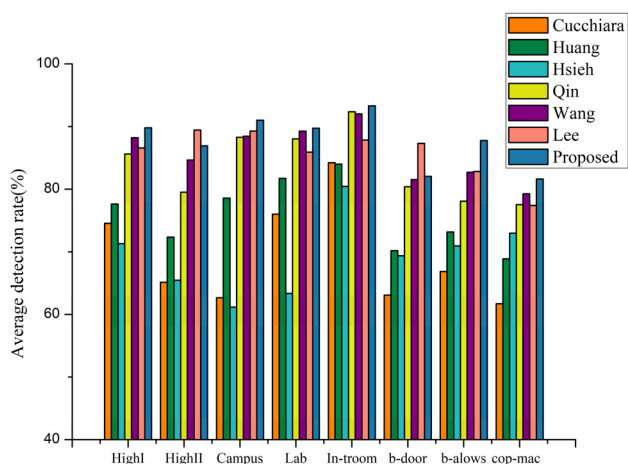


FIGURE 11. Average detection rate of the compared methods and the proposed.

proposed algorithm in this paper is slightly inferior in calculation time, there is still room for improvement.

VI. CONCLUSION

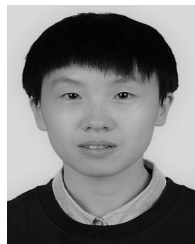
In this paper, we propose a novel method of moving object shadow elimination combined with dual-channel HSV color feature and UESILTP texture feature. According to the nature

of the shadow in terms of hue, brightness, saturation, and texture feature to minimize shadows. We use public videos set to validate different algorithms. The experimental results show that the proposed algorithm can gain ideal achievement for both strong and weak shadows. In the next work, we will strive to improve the calculation speed, such as use of parallel computing and so on. At the same time, we will try to use the knowledge of deep learning to solve the detection and elimination of moving shadows.

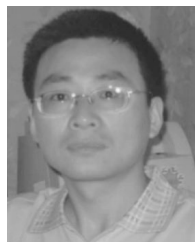
REFERENCES

- [1] C.-C. Chiu, M.-Y. Ku, and L.-W. Liang, "A robust object segmentation system using a probability-based background extraction algorithm," *IEEE Trans. Circuits Syst. Video Technol.*, vol. 20, no. 4, pp. 518–528, Apr. 2010.
- [2] W. He, Y. K.-W. Kim, H.-L. Ko, J. Wu, W. Li, and B. Tu, "Local compact binary count based nonparametric background modeling for foreground detection in dynamic scenes," *IEEE Access*, vol. 7, pp. 92329–92340, 2019.
- [3] S. Minaeian, J. Liu, and Y.-J. Son, "Effective and efficient detection of moving targets from a UAV's camera," *IEEE Trans. Intell. Transp. Syst.*, vol. 19, no. 2, pp. 497–506, Feb. 2018.
- [4] L. Z. Fang, W. Y. Qiong, and Y. Z. Sheng, "A method to segment moving vehicle cast shadow based on wavelet transform," *Pattern Recognit. Lett.*, vol. 29, no. 16, pp. 2182–2188, Dec. 2008.
- [5] A. Sanin, C. Sanderson, and B. C. Lovell, "Improved shadow removal for robust person tracking in surveillance scenarios," in *Proc. 20th Int. Conf. Pattern Recognit.*, Aug. 2010, pp. 141–144.
- [6] R. Cucchiara, C. Grana, M. Piccardi, and A. Prati, "Detecting moving objects, ghosts, and shadows in video streams," *IEEE Trans. Pattern Anal. Mach. Intell.*, vol. 25, no. 10, pp. 1337–1342, Oct. 2003.

- [7] J.-B. Huang and C.-S. Chen, "Moving cast shadow detection using physics-based features," in *Proc. IEEE Conf. Comput. Vis. Pattern Recognit.*, Jun. 2009, pp. 2310–2317.
- [8] C.-C. Chen and J. K. Aggarwal, "Human shadow removal with unknown light source," in *Proc. 20th Int. Conf. Pattern Recognit.*, Aug. 2010, pp. 2407–2410.
- [9] C.-T. Chen, C.-Y. Su, and W.-C. Kao, "An enhanced segmentation on vision-based shadow removal for vehicle detection," in *Proc. Int. Conf. Green Circuits Syst.*, Jun. 2010, pp. 679–682.
- [10] B. Sun and S. Li, "Moving cast shadow detection of vehicle using combined color models," in *Proc. Chin. Conf. Pattern Recognit. (CCPR)*, Oct. 2010, pp. 1–5.
- [11] M. Khare, R. K. Srivastava, and M. Jeon, "Shadow detection and removal for moving objects using Daubechies complex wavelet transform," *Multimedia Tools Appl.*, vol. 77, no. 2, pp. 2391–2421, Jan. 2018.
- [12] L. Zhang, Y. Cheng, Y. Xie, and L. Jie, "Shadow detection method in video sequences based on LBP," *J. Syst. Eng. Electron.*, vol. 6, no. 29, pp. 974–977, 2007.
- [13] A. Leone and C. Distanto, "Shadow detection for moving objects based on texture analysis," *Pattern Recognit.*, vol. 40, no. 4, pp. 1222–1233, Apr. 2007.
- [14] B. Wang and C. L. P. Chen, "Optical reflection invariant-based method for moving shadows removal," *Opt. Eng.*, vol. 57, no. 9, Sep. 2018, Art. no. 93102.
- [15] J.-W. Hsieh, W.-F. Hu, C.-J. Chang, and Y.-S. Chen, "Shadow elimination for effective moving object detection by Gaussian shadow modeling," *Image Vis. Comput.*, vol. 21, no. 6, pp. 505–516, Jun. 2003.
- [16] S. Nadimi and B. Bhanu, "Physical models for moving shadow and object detection in video," *IEEE Trans. Pattern Anal. Mach. Intell.*, vol. 26, no. 8, pp. 1079–1087, Aug. 2004.
- [17] A. J. Joshi and N. P. Papanikolopoulos, "Learning to detect moving shadows in dynamic environments," *IEEE Trans. Pattern Anal. Mach. Intell.*, vol. 30, no. 11, pp. 2055–2063, Nov. 2008.
- [18] W.-H. Xie, J.-Y. Zhao, and Y.-M. Hu, "Moving shadow detection algorithm using multiple features," in *Proc. Int. Conf. Comput. Sci. Appl. (CSA)*, Nov. 2015, pp. 95–98.
- [19] J. Dai, M. Qi, X. Yu, and J. Kong, "Integrated moving cast shadows detection method for surveillance videos," *Opt. Eng.*, vol. 11, no. 51, 2012, Art. no. 117005.
- [20] R. Qin, S. Liao, Z. Lei, and S. Z. Li, "Moving cast shadow removal based on local descriptors," in *Proc. 20th Int. Conf. Pattern Recognit.*, Aug. 2010, pp. 1377–1380.
- [21] A. Prati, I. Mikic, M. M. Trivedi, and R. Cucchiara, "Detecting moving shadows: Algorithms and evaluation," *IEEE Trans. Pattern Anal. Mach. Intell.*, vol. 25, no. 7, pp. 918–923, Jul. 2003.
- [22] P. Barcellos, V. Gomes, and J. Scharcanski, "Shadow detection in camera-based vehicle detection: Survey and analysis," *J. Electron. Imag.*, vol. 25, no. 5, May 2016, Art. no. 051205.
- [23] J. T. Lee, K.-T. Lim, and Y. Chung, "Moving shadow detection from background image and deep learning," in *Image and Video Technology*. Cham, Switzerland: Springer, 2016, pp. 299–306.
- [24] S. H. Khan, M. Bennamoun, F. Sohel, and R. Togneri, "Automatic feature learning for robust shadow detection," in *Proc. IEEE Conf. Comput. Vis. Pattern Recognit.*, Jun. 2014, pp. 1939–1946.
- [25] X. Hu, L. Zhu, C.-W. Fu, J. Qin, and P.-A. Heng, "Direction-aware spatial context features for shadow detection," in *Proc. IEEE/CVF Conf. Comput. Vis. Pattern Recognit.*, Jun. 2018, pp. 7454–7462.
- [26] Z. Zivkovic, "Improved adaptive Gaussian mixture model for background subtraction," in *Proc. 17th Int. Conf. Pattern Recognit. (ICPR)*, 2004, pp. 28–31.
- [27] Y. Yu, L. Kurniaggoro, and K.-H. Jo, "Moving object detection for a moving camera based on global motion compensation and adaptive background model," *Int. J. Control, Autom. Syst.*, vol. 17, no. 7, pp. 1866–1874, Jul. 2019.
- [28] S. K. Choudhury, P. K. Sa, S. Bakshi, and B. Majhi, "An evaluation of background subtraction for object detection Vis-a-Vis mitigating challenging scenarios," *IEEE Access*, vol. 4, pp. 6133–6150, 2016.
- [29] M. Russell, J. J. Zou, G. Fang, and W. Cai, "Feature-based image patch classification for moving shadow detection," *IEEE Trans. Circuits Syst. Video Technol.*, vol. 29, no. 9, pp. 2652–2666, Sep. 2019.
- [30] B. Wang, Y. Zhao, and C. L. P. Chen, "Moving cast shadows segmentation using illumination invariant feature," *IEEE Trans. Multimedia*, early access, Nov. 20, 2019, doi: 10.1109/TMM.2019.2954752.
- [31] Y. Yi, J. Dai, C. Wang, J. Hou, H. Zhang, Y. Liu, and J. Gao, "An effective framework using spatial correlation and extreme learning machine for moving cast shadow detection," *Appl. Sci.*, vol. 9, no. 23, p. 5042, 2019.
- [32] C. Stauffer and W. E. L. Grimson, "Adaptive background mixture models for real-time tracking," in *Proc. Proceedings. IEEE Comput. Soc. Conf. Comput. Vis. Pattern Recognit.*, Jun. 1999, pp. 246–252.



HONGRUI ZHANG was born in Xiaoyi, China. She received the master's degree in electronics and communication engineering from Northwest Normal University, Lanzhou, China, in 2018. She is currently pursuing the Ph.D. degree in radio physics with Central China Normal University, Wuhan, China. Her main research directions are in image processing and electronics.

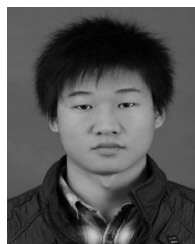


SHAOCHENG QU (Member, IEEE) received the B.Sc. degree in process control and instrument from the Wuhan University of Chemical and Technology, Wuhan, China, in 1994, the M.Sc. degree in control engineering from the Naval University of Engineering, Wuhan, in 2000, and the Ph.D. degree in control theory and control engineering from the Huazhong University of Science and Technology, Wuhan, in 2004. He is currently a Professor with Central China Normal University,

Wuhan, where he is also a Full Professor with the Department of Electronics and Information Engineering, College of Physical Science and Technology. He has provided consultancy to various industries. He has published over 70 articles on these topics. His main research interests are in the areas of control theory and applications, embedded systems, the IoT system applications, and intelligent information processing and control.



HUAN LI was born in Baoji, China. She received the master's degree in electronics and communication engineering from Northwest Normal University, Lanzhou, China, in 2018. She is currently with the Army Special Operations College. Her main research directions are in image processing and optical communication.



JING LUO received the B.Sc. degree from the Hubei University of Science and Technology, China, in 2012, and the M.Sc. degree in IC engineering from the School of Electronic Information, Wuhan University, China, in 2015. He is currently pursuing the Ph.D. degree with the Department of Electronics and Information Engineering, Central China Normal University, Wuhan, China. His research interests are in chaotic systems, memristor systems, and finite time control.



WENJUN XU was born in Jingzhou, China. He received the B.Sc. degree in biomedical engineering from the Hubei University of Economics, Wuhan, China, in 2013, and the M.Sc. degree in signal and information processing from Central China Normal University, Wuhan, in 2017, where he is currently pursuing the Ph.D. degree with the Department of Electronics and Information Engineering. His main research interests include design and control of motor drive, power electronics, intelligent control, and energy control.

...